



HAL
open science

Numerical investigation of contact/impact problems between deformable bodies

Benoit Magnain, Zhi-Qiang Feng, Jean-Michel Cros

► **To cite this version:**

Benoit Magnain, Zhi-Qiang Feng, Jean-Michel Cros. Numerical investigation of contact/impact problems between deformable bodies. 6th European Conference on Structural Dynamics (Eurodyn 2005), European Association for Structural Dynamics, Sep 2005, Paris, France. hal-01825988

HAL Id: hal-01825988

<https://hal.science/hal-01825988>

Submitted on 28 Jun 2018

HAL is a multi-disciplinary open access archive for the deposit and dissemination of scientific research documents, whether they are published or not. The documents may come from teaching and research institutions in France or abroad, or from public or private research centers.

L'archive ouverte pluridisciplinaire **HAL**, est destinée au dépôt et à la diffusion de documents scientifiques de niveau recherche, publiés ou non, émanant des établissements d'enseignement et de recherche français ou étrangers, des laboratoires publics ou privés.

Numerical investigation of contact/impact problems between deformable bodies

B. Magnain, Z.-Q Feng, J.-M. Cros

Laboratoire de Mécanique et d'Énergétique d'Évry, Université d'Évry Val d'Essonne

ABSTRACT: The bi-potential method has been successfully applied to the modelling of frictional contact problems in static cases. This paper presents the extension of this method for dynamic analysis of impact problems. A first order algorithm is applied to the numerical integration of the time-discretized equation of motion. The solution algorithm is simple and efficient. Two numerical examples are carried out in 2D: a longitudinal elastic impact between two slender bars and a more complex impact between two cylinders inside rigid walls.

1 INTRODUCTION

Problems involving contact and friction are among the most difficult ones in mechanics and at the same time of crucial practical importance in many engineering branches. The main mathematical difficulty lies in the severe contact non-linearities because the natural first order constitutive laws of contact and friction phenomena are expressed by non-smooth multivalued force-displacement or force-velocity relations. A large number of algorithms for the numerical solution of the related equations and inequalities have been presented in literature. The popular penalty method appears, at first glance, suitable for many applications. But in this method, the contact boundary conditions and friction laws are not accurately satisfied and it is difficult for the users to choose appropriate penalty factors. In addition, it may fail for stiff problems because of unpleasant numerical oscillations between contact statuses. In mutually independent works, Alart and Curnier (1991) and Simo and Laursen (1992) have proposed the augmented Lagrangian method. De Saxcé and Feng (1998) have proposed another augmented Lagrangian formulation and the bi-potential method, which is somewhat different from the one presented in the first two works. In particular, the frictional contact problem is treated in a reduced system by means of a predictor-corrector solution algorithm. In addition, the bi-potential method leads to a single displacement variational principle and a unique inequality in which the unilateral contact and the friction are coupled via a contact bi-potential. Using the bi-potential properties, the application of the augmented Lagrangian method to the contact laws

leads to an equation of projection onto Coulomb's cone, strictly equivalent to the original inequality.

Usually, the time-discretized equation of motion of dynamic system is integrated by second order algorithms such as Newmark, Wilson, etc. In this kind of methods, the acceleration is often assumed to be constant or to vary linearly within one time step. However, it is well known that in impact problems, the velocity and acceleration are not continuous because of the sudden changes in contact conditions. So the second order algorithms may lead to serious errors (1998). In this work we use the first order integration algorithm proposed by Jean (1989) in which the acceleration doesn't need to be calculated. The total Lagrangian formulation is used to take into account the large displacements and rotations that occur in impact problems.

In the present paper, we propose an extension of the bi-potential method for the modelling of impact problems using a first order algorithm for integration of the equation of motion. Two numerical examples are performed in this study to show the validity of the model developed. The first example concerns the longitudinal impact between two elastic bars. The second example simulates the impact of two elastic cylinders in rigid walls.

2 THE BI-POTENTIAL METHOD

In the following section, basic definitions and notations used are described. Two deformable bodies \mathcal{B}^α (Figure 1), $\alpha = 1, 2$, are considered. Each of them occupies the open, simply connected, bounded do-

main $\Omega^\alpha \subset \mathbb{R}^3$, whose generic point is denoted \mathbf{X}^α . Furthermore, the solids are elastic and undergo large displacements. The boundary Γ^α of each body is assumed to be sufficiently smooth everywhere so that an outward unit normal vector, denoted by \mathbf{n}^α , can be defined at any point M on Γ^α . At each time $t \in \mathbf{I}$, where $\mathbf{I} = [0, T]$ denotes the time interval corresponding to the loading process, the boundary Γ^α of the body \mathcal{B}^α can, in general, be split into three parts: Γ_u^α with prescribed displacements $\bar{\mathbf{u}}^\alpha$, Γ_t^α with prescribed boundary loads $\bar{\mathbf{t}}^\alpha$, and the potential contact surfaces Γ_c^α where the two bodies \mathcal{B}^1 and \mathcal{B}^2 may possibly come into contact at some time t :

$$\Gamma^\alpha = \Gamma_u^\alpha \cup \Gamma_t^\alpha \cup \Gamma_c^\alpha \quad (1)$$

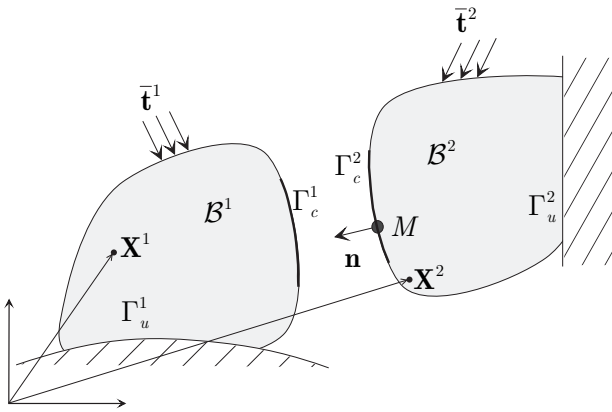


Figure 1. Contact kinematics

The successive deformed configurations of \mathcal{B}^α are described at each time t by the displacement fields \mathbf{u}^α defined on Ω^α). On the contact surface, a unique normal \mathbf{n} directed towards \mathcal{B}^1 ($\mathbf{n} \equiv \mathbf{n}^2$) is defined and the tangential plane, orthogonal to \mathbf{n} in \mathbb{R}^3 , is denoted by \mathbf{T} . To construct a local basis, two unit vectors \mathbf{t}_x and \mathbf{t}_y are defined within the plane \mathbf{T} . For describing the frictional contact interactions that may occur on Γ_c , we introduce the relative velocity with respect to \mathcal{B}^2

$$\dot{\mathbf{u}} = \dot{\mathbf{u}}^1 - \dot{\mathbf{u}}^2 \quad (2)$$

where $\dot{\mathbf{u}}^1$ and $\dot{\mathbf{u}}^2$ are the instantaneous velocities of \mathcal{B}^1 and \mathcal{B}^2 . Let \mathbf{r} be the contact force distribution exerted on \mathcal{B}^1 at M from \mathcal{B}^2 . According to the action-reaction principle, \mathcal{B}^2 is subjected to $-\mathbf{r}$. In the local coordinate system defined by the tangential plane \mathbf{T} and the normal \mathbf{n} , any element $\dot{\mathbf{u}}$ and \mathbf{r} may be uniquely decomposed as

$$\dot{\mathbf{u}} = \dot{\mathbf{u}}_t + \dot{u}_n \mathbf{n}, \quad \dot{\mathbf{u}}_t \in \mathbf{T}, \quad \dot{u}_n \in \mathbb{R} \quad (3)$$

$$\mathbf{r} = \mathbf{r}_t + r_n \mathbf{n}, \quad \mathbf{r}_t \in \mathbf{T}, \quad r_n \in \mathbb{R} \quad (4)$$

The unilateral contact law is characterized by a geometric condition of non-penetration, a static condition of no-adhesion and a mechanical complementary

condition. These three conditions are known as the Signorini conditions:

$$u_n \geq 0, \quad r_n \geq 0, \quad u_n r_n = 0 \quad (5)$$

In case of dynamic analysis such as impact problems, the Signorini conditions can be formulated, in terms of relative velocity:

$$\dot{u}_n \geq 0, \quad r_n \geq 0, \quad \dot{u}_n r_n = 0 \quad (6)$$

Classically, a rate independent dry friction law is characterized by a kinematic slip rule. In this work, the classical Coulomb friction rule is used. The set of admissible forces, denoted by K_μ , is defined by:

$$K_\mu = \{ \mathbf{r} \in \mathbb{R}^3 \text{ such that } \|\mathbf{r}_t\| - \mu r_n \leq 0 \} \quad (7)$$

K_μ is the so-called Coulomb's cone and is convex. De Saxcé and Feng (1998) have introduced the bi-potential defined by:

$$b_c(-\dot{\mathbf{u}}, \mathbf{r}) = \bigcup_{\mathbb{R}_-} (-\dot{u}_n) + \bigcup_{K_\mu} (\mathbf{r}) + \mu r_n \|\dot{\mathbf{u}}_t\| \quad (8)$$

where $\mathbb{R}_- =]-\infty, 0]$ is the set of the negative and null real numbers and $\bigcup_{K_\mu} \mathbf{r}$ denotes the so-called indicator function of the closed convex set K_μ :

$$\bigcup_{K_\mu} (\mathbf{r}) = \begin{cases} 0 & \text{if } \mathbf{r} \in K_\mu \\ +\infty & \text{otherwise} \end{cases} \quad (9)$$

In order to avoid nondifferentiable potentials that occur in nonlinear mechanics, such as in contact problems, it is convenient to use the augmented Lagrangian method. For the contact bi-potential b_c , given by (8), provided that $\dot{u}_n \geq 0$ and $\mathbf{r} \in K_\mu$, we have:

$$\forall \mathbf{r}' \in K_\mu : \quad \varrho \mu (r'_n - r_n) \|\dot{\mathbf{u}}_t\| + (\mathbf{r} - (\mathbf{r} - \varrho \dot{\mathbf{u}})) \cdot (\mathbf{r}' - \mathbf{r}) \geq 0 \quad (10)$$

where ϱ is a solution parameter which is not user-defined. In order to ensure numerical convergence, ϱ can be chosen as the maximum value of the diagonal terms of the local contact stiffness matrix. Taking account of the decomposition (3,4), the following inequality has to be satisfied:

$$\mathbf{r}' \in K_\mu, \quad (\mathbf{r} - \boldsymbol{\tau}) \cdot (\mathbf{r}' - \mathbf{r}) \geq 0 \quad (11)$$

where the modified augmented surface traction $\boldsymbol{\tau}$ is defined by

$$\boldsymbol{\tau} = \mathbf{r} - \varrho (\dot{\mathbf{u}}_t + (\dot{u}_n + \mu \|\dot{\mathbf{u}}_t\|) \mathbf{n}) \quad (12)$$

The inequality (11) means that \mathbf{r} is the projection of $\boldsymbol{\tau}$ onto the closed convex Coulomb's cone:

$$\mathbf{r} = \text{proj}(\boldsymbol{\tau}, K_\mu) \quad (13)$$

To find the numerical solution of the implicit equation (13), Uzawa's algorithm can be used, which leads to an iterative process involving one predictor-corrector step:

$$\begin{aligned} \text{Predictor } \boldsymbol{\tau}^{i+1} &= \mathbf{r}^i - \rho^i (\dot{\mathbf{u}}_t^i + (\dot{u}_n^i + \mu \|\dot{\mathbf{u}}_t^i\|) \mathbf{n}) \\ \text{Corrector } \mathbf{r}^{i+1} &= \text{proj}(\boldsymbol{\tau}^{i+1}, K_\mu) \end{aligned} \quad (14)$$

It is worth noting that, in this algorithm, the unilateral contact and the friction are coupled via the bi-potential. Another gist of the bi-potential method is that the corrector can be analytically found with respect to the three possible contact statuses: $\boldsymbol{\tau} \subset K_\mu$ (contact with sticking), $\boldsymbol{\tau} \subset K_\mu^*$ (no contact) and $\boldsymbol{\tau} \subset \mathbb{R}^3 - K_\mu \cup K_\mu^*$ (contact with sliding). K_μ^* is the polar cone of K_μ . It is important to emphasize the fact that this explicit formula is valid for both 2D and 3D contact problems with Coulomb's friction and allows us to obtain very stable and accurate results.

3 FINITE ELEMENT FORMULATION OF NON-LINEAR STRUCTURES

3.1 Total Lagrangian formulation

In order to describe the geometrical transformation problems, we use the deformation gradient tensor:

$$\mathbf{F} = \mathbf{Id} + \nabla \mathbf{u} \quad (15)$$

where \mathbf{Id} is the unity tensor and $\nabla \mathbf{u}$ the displacement gradient tensor. Because of large displacements and rotations, Green-Lagrangian strain is adopted for the nonlinear relationships between strains and displacements. We note \mathbf{C} the stretch tensor or the right Cauchy-Green deformation tensor ($\mathbf{C} = \mathbf{F}^T \mathbf{F}$). The Green-Lagrangian strain tensor \mathbf{E} is defined by:

$$\mathbf{E} = \frac{1}{2}(\mathbf{C} - \mathbf{I}) \quad (16)$$

In the context of the finite element method and from Eqs.(15, 16), the Green-Lagrangian strain includes formally linear and nonlinear terms in function of nodal displacements:

$$\mathbf{E} = \left(\mathbf{B}_L + \frac{1}{2} \mathbf{B}_{NL}(\mathbf{u}) \right) \mathbf{u} \quad (17)$$

where \mathbf{B}_L is the matrix which relates the linear strain term to the nodal displacements, and $\mathbf{B}_{NL}(\mathbf{u})$, the matrix which relates the nonlinear strain term to the nodal displacements. In the particular case of isotropic Saint-Venant-Kirchhoff material models, we have:

$$\mathbf{S} = \mathbf{D} : \mathbf{E} \quad (18)$$

where \mathbf{D} and \mathbf{S} respectively denote the usual material secant tangent and the second Piola-Kirchhoff stress

tensor. Using the finite element method, the equilibrium equation for an impact problem can be generally written in the form:

$$\mathbf{M}\ddot{\mathbf{u}} + \mathbf{C}\dot{\mathbf{u}} + \mathbf{F}_{int} - \mathbf{F}_{ext} - \mathbf{R}_c = 0 \quad (19)$$

where \mathbf{F}_{ext} , \mathbf{F}_{int} and \mathbf{R}_c are respectively the external, internal and contact forces. In this equation, reaction forces are introduced like a second type of external forces. \mathbf{M} is the mass matrix and \mathbf{C} is the damping matrix. $\ddot{\mathbf{u}}$ is the acceleration vector and $\dot{\mathbf{u}}$ is the velocity vector. It is noted that the stiffness effect is taken into account by the internal forces vector \mathbf{F}_{int} . Taking the derivative of \mathbf{F}_{int} with respect to the nodal displacements \mathbf{u} gives the tangent stiffness matrix as

$$\mathbf{K} = \frac{\partial \mathbf{F}_{int}}{\partial \mathbf{u}} = \mathbf{K}_e + \mathbf{K}_\sigma + \mathbf{K}_u \quad (20)$$

The tangent stiffness matrix is in fact the sum of the elastic stiffness matrix \mathbf{K}_e , the geometric stiffness (or initial stress stiffness) matrix \mathbf{K}_σ and the initial displacement stiffness matrix \mathbf{K}_u :

$$\mathbf{K}_e = \int_{V_0} \mathbf{B}_L^T \mathbf{D} \mathbf{B}_L dV \quad (21)$$

$$\mathbf{K}_\sigma = \int_{V_0} \mathbf{S} \frac{\partial \mathbf{B}_{NL}}{\partial \mathbf{u}} dV \quad (22)$$

$$\mathbf{K}_u = \int_{V_0} (\mathbf{B}_L^T \mathbf{D} \mathbf{B}_{NL} + \mathbf{B}_{NL}^T \mathbf{D} \mathbf{B}_L + \mathbf{B}_{NL}^T \mathbf{D} \mathbf{B}_{NL}) dV \quad (23)$$

where V_0 is the volume of the initial configuration.

3.2 First-order algorithm

For the integration of Eq.(19), we adopt a first-order algorithm based on the following velocity approximation (Jean 1989):

$$\dot{\mathbf{u}} = \frac{\mathbf{u}^{t+\Delta t} - \mathbf{u}^t}{\Delta t} = (1 - \theta) \dot{\mathbf{u}}^t + \theta \dot{\mathbf{u}}^{t+\Delta t} \quad (24)$$

with ($0 \leq \theta \leq 1$). Then, we obtain the following Newton-Raphson iterative formulation:

$$\begin{cases} \bar{\mathbf{K}}^i \Delta \mathbf{u} &= \bar{\mathbf{F}}^i + \bar{\mathbf{F}}_{acc}^i + \mathbf{R}_c^{i+1} \\ \mathbf{u}^{i+1} &= \mathbf{u}^i + \Delta \mathbf{u} \end{cases} \quad (25)$$

where $\bar{\mathbf{K}}^i$, $\bar{\mathbf{F}}_{acc}^i$ and $\bar{\mathbf{F}}^i$ are calculated by ($0 \leq \xi \leq 1$):

$$\begin{cases} \bar{\mathbf{K}}^i &= \xi \mathbf{K}^i + \frac{\xi}{\theta \Delta t} \mathbf{C}^i + \frac{1}{\theta \Delta t^2} \mathbf{M}^i \\ \bar{\mathbf{F}}_{acc}^i &= -\frac{1}{\theta \Delta t^2} \mathbf{M}^i \{ \mathbf{u}^i - \mathbf{u}^t - \Delta t \dot{\mathbf{u}}^t \} \\ \bar{\mathbf{F}}^i &= (1 - \xi)(\mathbf{F}_{int}^t + \mathbf{F}_{ext}^t) + \xi(\mathbf{F}_{int}^i + \mathbf{F}_{ext}^{t+\Delta t}) \end{cases} \quad (26)$$

At the end of each time step, the velocity is updated by:

$$\dot{\mathbf{u}}^{t+\Delta t} = (1 - \frac{1}{\theta}) \dot{\mathbf{u}}^t + \frac{1}{\theta \Delta t} (\mathbf{u}^{t+\Delta t} - \mathbf{u}^t) \quad (27)$$

In the following numerical results, the local velocity at the contact interfaces are expressed in terms of the average velocity over a time step:

$$\bar{\mathbf{u}} = (1 - \theta) \dot{\mathbf{u}}^t + \theta \dot{\mathbf{u}}^{t+\Delta t} \quad (28)$$

4 NUMERICAL RESULTS

The algorithms presented above have been implemented and tested in the finite element code FER/Impact. To illustrate the effectiveness and the robustness of the algorithm, we consider two example applications which are homogenous Neumann problems (no displacements or external forces imposed). For both cases, we assume that no damping exists except for Coulomb friction between contact surfaces, *i.e.* $\mathbf{C} = 0$ in Eqs.(19, 26). Moreover, the algorithm parameters used for the following simulation are $\theta = \xi = 0.5$ for which the first order algorithm is conservative. Dimensionless data are intentionally used for these analyses.

4.1 Longitudinal elastic impact

The first example of dynamics is presented in order to verify the validity and the efficiency of the method developed. The problem concerns the longitudinal impact of two elastic bars in 2D. Two cases are considered : impact between similar and dissimilar bars. Geometric configurations and material characteristics of the two considered cases are reported in Figure 2 and Table 1.

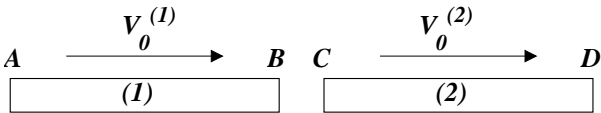


Figure 2. Longitudinal impact of two elastic bars

Table 1. Material and geometric data

	case 1		case 2	
T	0.04		50.0	
Δt	0.00001		0.01	
	bar (1)	bar (2)	bar (1)	bar (2)
Length	10	10	100	100
E	1000	1000	10,000	80,000
ρ	0.001	0.001	100	200
V_0	1.0	-1.0	0.1	0.0

4.1.1 Case 1: similar bars

For this first simulation, both bars have the same material properties. For each of the following displayed results, analytical solutions are plotted in order to check the efficiency of the proposed method. In Figure 3 the nodal displacement of point C is plotted. It shows a good concordance between the analytical solution and the numerical solution.

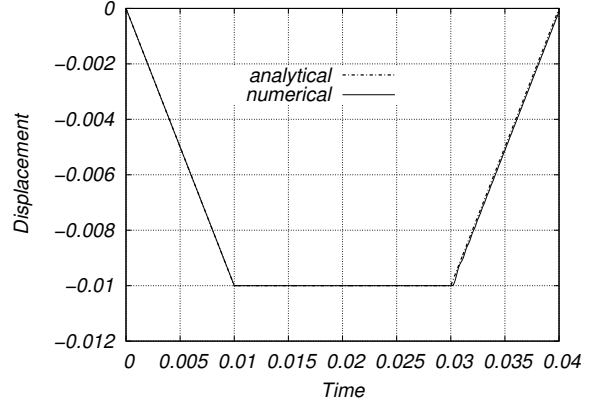


Figure 3. Local displacement of point C

The velocities and reaction forces at the contact interface (point C) are plotted in Figures 4 and 5.

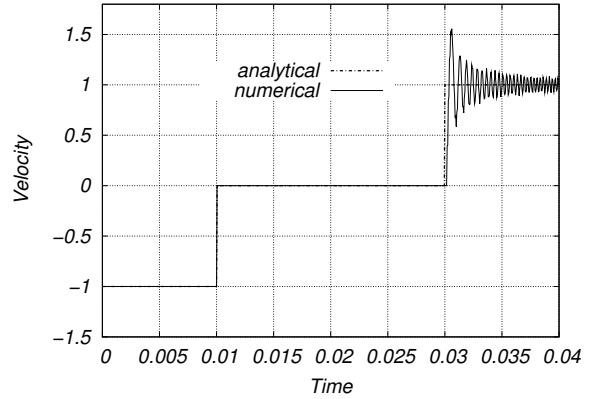


Figure 4. Local velocity of point C

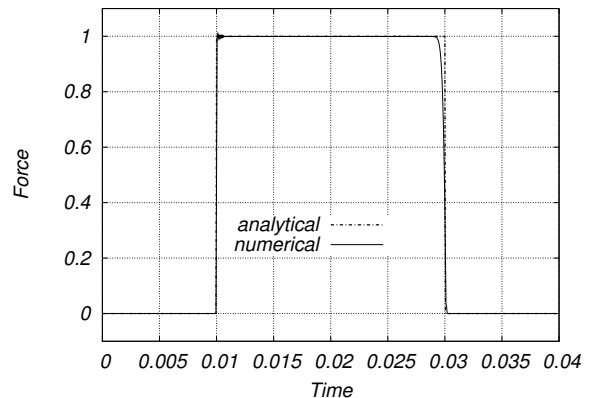


Figure 5. Reaction force of point C

Figure 6 displays the energy evolution of the full system (bar(1) + bar(2)). E_k , E_e and $E_t = E_k + E_e$ are respectively the kinetic energy, the elastic strain energy and the total energy. It shows that the proposed method permits us to verify the principle of energy conservation for frictionless contact problems.

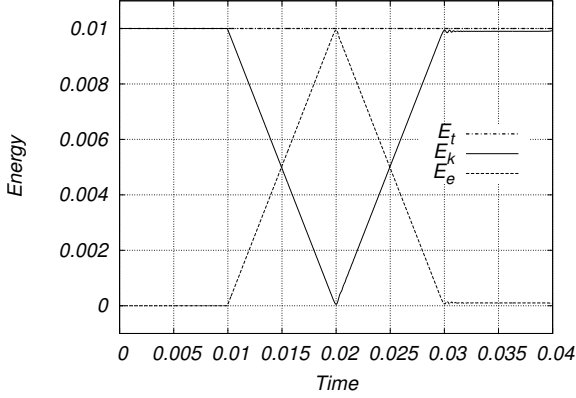


Figure 6. Energy evolution

4.1.2 Case 2: dissimilar bars

This example has been first studied by Laursen and Love (2002) with a penalty regularization method. The displacements of both bars and the local velocities at the contact interface are plotted in Figures 7 and 8.

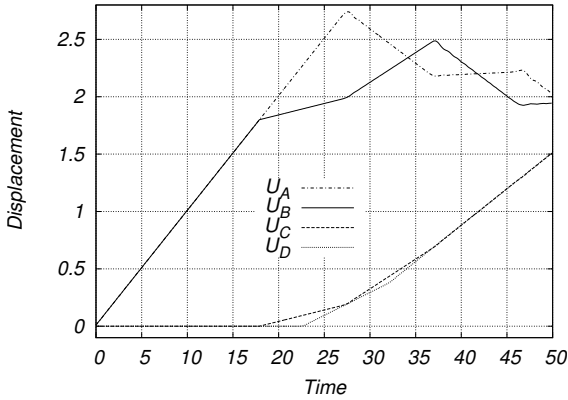


Figure 7. Local displacements

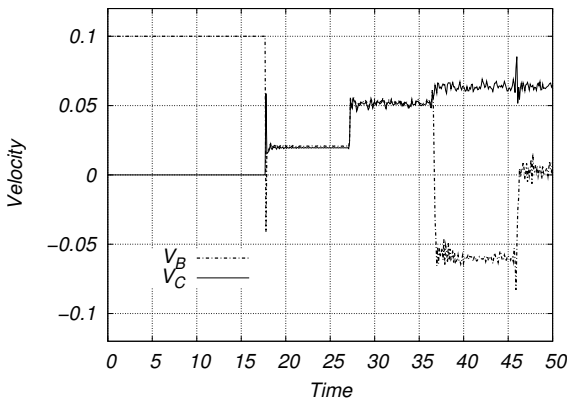


Figure 8. Velocity at the contact interface

For each bar, the evolution of total energy is plotted in Figure 9. Once again, the total energy of the system ($E_t = E_{t_1} + E_{t_2}$) is conserved.

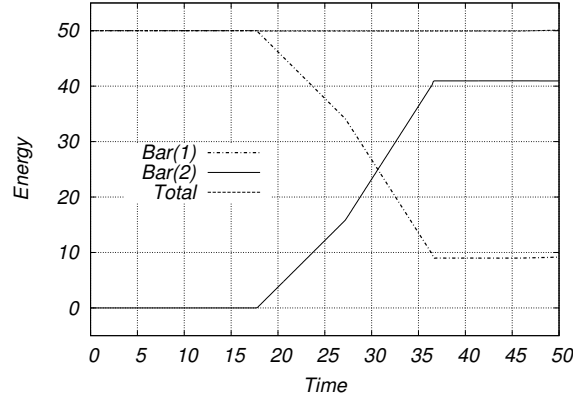


Figure 9. Energy evolution ($\mu = 0.0$)

4.2 Impact of two cylinders inside rigid walls

The second example is dealing with the impact of two elastic cylinders inside rigid walls. This problem, proposed by Armero and Petocz (1998), permits to explore the performance of the presented method in the case of deformable-deformable contact. The geometric data of the problem is displayed in Figure 10. The material constants of the both cylinders are : $E = 2700$, $\nu = 0.33$, and $\rho = 1$. The left cylinder is given an initial velocity of $V_x = 1.0$ and $V_y = -2.0$, hitting the bottom rigid wall and afterwards the right cylinder as depicted in Figure 10. The total simulation time is 15 and time step is $\Delta t = 10^{-3}$.

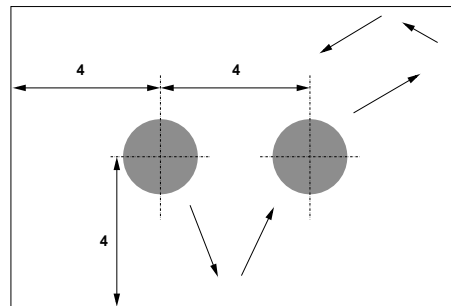


Figure 10. Impact of two cylinders inside rigid walls

In Figures 11 and 12, E_t , E_k and E_e are plotted in the case of frictionless ($\mu = 0.0$) and frictional ($\mu = 0.2$) contact. We can clearly observe that the total energy is quite well conserved in the case of frictionless contact. However, in the case of frictional contact ($\mu = 0.2$), the total energy decreases at each shock (Figure 12). As expected, the energy is dissipated by frictional effects.

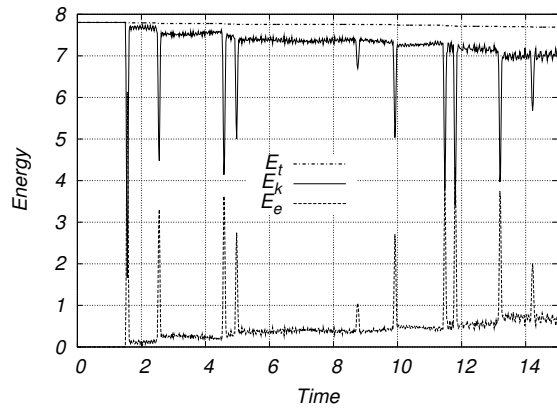


Figure 11. Energy evolution ($\mu = 0.0$)

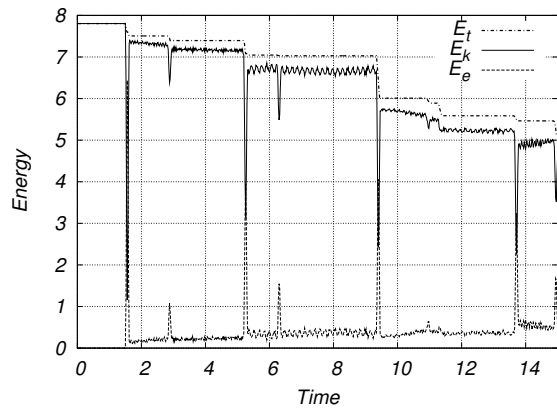


Figure 12. Energy evolution ($\mu = 0.2$)

Figure 13 shows the distribution of the shear stress of the left cylinder when it hits the bottom wall. As expected, the distribution is symmetrical in frictionless case while this is not true in frictional case.

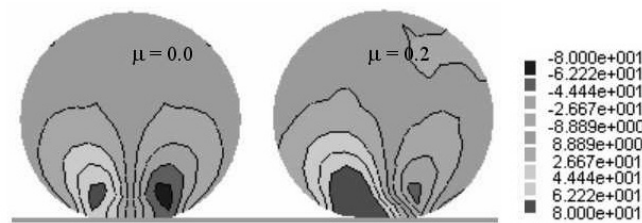


Figure 13. Distribution of shear stress at $t = 1.56$ s

5 CONCLUSION

In this paper, we have presented the recent development of the bi-potential method applied to dynamic analysis in impact mechanics. The numerical algorithms are described. The presented results demonstrate that the proposed method can provide good results in terms of numerical stability and precision. The proposed algorithms seem to preserve the total energy of the system in the case of frictionless contact and also take into account the physical energy dissipation by frictional effects.

REFERENCES

- Alart, P. & Curnier, A. 1991. A mixed formulation for frictional contact problems prone to newton like solution methods. *Comp. Meth. Appl. Mech. Engng.* 92, 353–375.
- Armero, F. & Petocz, E. 1998. Formulation and analysis of conserving algorithms for frictionless dynamic contact/impact problems. *Comp. Meth. Appl. Mech. Engng.* 158, 269–300.
- De Saxcé, G. & Feng, ZQ. 1998. The bi-potential method: a constructive approach to design the complete contact law with friction and improved numerical algorithms. *Mathematical and Computer Modeling* 28(4-8), 225–245. special issue Recent Advances in Contact Mechanics.
- Jean, M. 1989. Dynamics with partially elastic shocks and dry friction: double scale method and numerical approach. *4th Meeting on unilateral problems in structural analysis.* Capri.
- Laursen, TA. & Love, GR. 2002. Improved implicit integrators for transient impact problems geometric admissibility within the conserving framework. *Int. J. Num. Meth. Engng.* 53, 245–274.
- Simo, JC. & Laursen, TA. 1992. An augmented lagrangian treatment of contact problems involving friction. *Computers & Structures* 42, 97–116.